CRACK HEALING IN CEMENTITIOUS MATERIALS INCLUDING TESTS METHODS

Alan Elliott Richardson,[1] Brabha Nagaratnam,[2] Kathryn Ann Coventry,[3]
Dominic Brandy,[4] Leon Amess[5]

ABSTRACT

If concrete is crack free, deleterious substances can be avoided entering the body of the material, that may corrode the rebar or encourage freeze/thaw damage. This paper examines a self healing system of cementitious materials.

Microbial induced calcite precipitation was used to heal cracks in concrete with calcite using bacillus bacteria in alkaline conditions to generate a calcite filling material.

Self healing of cracked prisms was determined using a water flow and absorption test and the results were expressed to record the healing as a percentage.

The findings of the tests showed that a significant degree of self healing had taken place after 56 days after inducing a crack to the concrete prisms and the water flow test was appropriate to determine the degree of self healing taking place.

Limitations of this process are such that the process requires a biological laboratory to create the spore impregnated aggregate. Once the aggregate is prepared, the batching process is essentially the same as any normal concrete.

A practical use of this system could be developed using cover panels of self healing material to act as permanent formwork, thus placing the healing ingredients where they are needed at a minimum cost. The system has huge potential for the creation of a self repairing sustainable infrastructure.

KEYWORDS

Alkaphillic bacteria, concrete, sustainability, strength, water flow, water absorption, calcite

1.0 INTRODUCTION

Deterioration of cementious materials is inevitable. The need for concrete repairs through the service life of concrete works has given rise to the development of various surface treatments which vary in their application, finish and the properties they imbue to the repair-work (Barbero-Barrera et al, 2013). Options for remedial treatments are: render coatings, resin coating, epoxy treatments and sprayed concrete and all methods strive to re-instate the appearance of the

1. Engineering and Environment, Northumbria University, UK, arichardson@northumbria.ac.uk
2. Engineering and Environment, Northumbria University, UK
3. School of Mathematics Department, UEA ,UK
4. Engineering and Environment, Northumbria University, UK
5. Engineering and Environment, Northumbria University, UK

concrete's cementitious finish. However, many of these techniques are expensive, detrimental to the environment and difficult to apply. A very common factor contributing to deterioration in concrete is that of crack formation (Wiktor and Jonkers, 2011). Euro Code 2, permits 0.3 mm wide cracks, at the surface of a structural member. Cracks increase permeability allowing water ingress and potentially deleterious substances to gain access to the internal structure of the concrete, thereby accelerating deterioration and sustainability is reduced (Pacheco-Torgal and Labrincha, 2013). This reduction in sustainability is due to damage caused by entry of water to the interior of the concrete, permitting freeze/thaw crack initiation and propagation, which in turn may lead to spalling of the structure, thus exposing the rebar to the elements, which in turn may lead to galvanic action and oxidation of the steel rebar, constituting a lower life cycle structure. Autogenous healing is a phenomenon that is applicable to small cracks up to 50 microns in width; larger cracks need alternative forms of repair. Sealing larger cracks is possible, however, "most sealing agents are based on organic polymers which have some degree of toxicity. There is a need for a reduction in toxic materials in construction" as indicated in Regulation (EU) 305/2011. (Pacheco-Torgal and Labrincha, 2013, pp. 1136–1136). This paper presents an alternative approach to crack repairs in concrete using a bacteria first observed by Brown in 1886 (Brown 1886), who described the acetobacter xylinum bacteria and its ability to grow and thrive, while assuming unique physical properties (Matsuoka et al,1996). Hitherto, the potential to explore the adoption of bacterial technology repair in concrete works was prevented due to low bacterial production yields. However, with the potential for improved bacterial yields and the associated reduction in price; research into bacteria repair technology in concrete works is feasible and is producing encouraging results.

By being able to repair cracks through the use of natural ground borne bacteria, *Bacillus sphaericus* (LMG 22257) reduces toxins in the repaired material when compared to chemical repair systems. The bacteria as used, is classed as a biohazard group 1 and consists of organisms that are unlikely to cause human disease and can be handled under containment level 1. They can also be distributed unrestrictedly to any bona fide teaching, research or industrial institution making them widely suitable for repairing concrete. Schramm et al, (2004) explain that due to the manufacturing process of 'man-made' sealants, some of which contain petroleum based compounds, the repair product can cause potential respiratory issues if used internally. Furthermore, the leakage or improper disposal of such petroleum based sealants could cause severe damage to the natural environment.

The idea of self-healing concrete has been around since the 1990's. Gollapudi et al., (1995) suggest the introduction of ureolytic bacteria which helps with the precipitation of calcium calcite, (Wu, et al., 2012) which seals cracks. Jonkers (2010) argues that the bacteria used is suitable for the life time of the building and is able to perform effective crack sealing. The bacteria act as a catalyst to a precursor, which in turn creates a bio-cement calcite filling any cracks that form. Jonkers (2010) showed that the precursor compound had to be organic for the effective life span to be suitable. Calcium lactate is a suitable precursor due to the strength of the concrete mix not being affected when incorporated. Furthermore, a different bio mineralisation process occurred compared to the ureolytic processes.

2.0 BACTERIAL STRAIN AND TEST PROGRAMME

A strain of alkaphilic spore forming bacteria, *Bacillus sphaericus* (LMG 22257) was used in this study to investigate its efficacy in the repair of concrete work. The spores used in this paper are

known to be able to withstand the high mechanical forces of mixing into a concrete mix and the pH of 11 to 13 associated with fresh concrete (Jonkers et al. 2010). This strain of bacteria precipitates calcium carbonate ($CaCO_3$) onto its cell constituents and in its micro-environment, by the process of mineral formation from calcium lactate. Calcium lactate does not reduce the strength of the concrete unlike calcium acetate and yeast extract when used in urease systems. The metabolic bacterial conversion of calcium lactate to calcium carbonate according to Jonkers et al. (2010) is:

$$CaC_6H_{10}O_6 + 6O_2 \rightarrow CaCO_3 + 5CO_2 + 5H_2O \quad \text{[Eq 1]}$$

This represents an alternative mechanism to the urease based systems, previously used, with the advantage that ammonia is not produced in massive amounts. Ammonia can cause rebar corrosion. (Jonkers et al. 2010). The latter subsequently promotes the microbial deposition of $CaCO_3$ in a calcium rich environment. Through this process, the bacterial cell is coated with a layer of $CaCO_3$. This bio-$CaCO_3$ has been explored (Wiktor and Jonkers 2011) for the protection of cementitious materials and natural stone to improve the durability. The bio deposition treatment consisted of two laboratory steps: (i) creation of a bacterial grown culture and (ii) the addition of bacteria to a nutrient broth medium with precipitation precursors. Bio-deposition treatment resulted in the presence of a layer of $CaCO_3$ crystals.

The test programme adopted in this study aimed to demonstrate evidence of crack healing for bacterial concrete mixes. The study compared control concrete samples against those in which bacteria is encouraged to grow, as well as concrete with a food source only to determine the effect of the food source on the hardened concrete. Through the consideration of water volumes flowing through a cracked concrete prism, tested prior to and post bacterial healing, this study deemed it possible to determine evidence of concrete repair. Further to this, scanning electron microscopy (SEM) and three-dimensional fracture measurements provided images for supporting the analysis of the repaired concrete crack.

2.1 Test sample—mix specification and preparation.

Three mixes were designed to enable the production of test prisms of dimensions; length (l): (160 ±1) mm; width (b): (40.0 ± 0.1) mm; and depth (h): (40.0 ± 0.1) mm. These dimensions are in accordance with BS EN 1015-11 and are reflective of those samples adopted by other researches (Wiktor and Jonkers 2011). The test prisms had a central 5 mm diameter hole running longitudinally for the full length and two 1 mm diameter wire reinforcement to hold the prism together once an induced crack was created under three point loading configuration. A central notch was cut into the base of each prism 2 mm deep. The induced crack was measured after tensile recovery of the material following the release of the central point load.

The basic mix design of each concrete sample, detailed in this section, assumed a mortar mix manufactured in accordance with EN 196-1. Each basic mix utilised the pervious Liapor clay aggregate within the design to ensure consistency, however, the voids within this aggregate afforded potential sites into which bacterial spores could be absorbed.

Liapor is a round clay expanded clay aggregate with a bulk density of 450 kg/m^3 and when subject to immersion in water, is subject to an 11% by mass, water absorption over a 24 hours period of time. The aggregate production process requires clay to be sintered to a heat (1100–1200°C) where gasses are produced (bloating) in the pyro plastic clay body and this expands to produce a fine honeycomb texture. The control mix, containing no bacteria, was

TABLE 1. Mortar Composition for all mix designs.

Mix Ingredients	Weight (g)	Mix N—control mix	Mix R—mix and food source	Mix BAC—mix, bacteria and food
Cement (CEM I 42.5)	450	*	*	*
Sand 0–2 mm	1350	*	*	*
Water (potable)	225 (0.225L)	*	*	*
Food Source Calcium lactate at 15g/100 mm^3	11.52		*	
Impregnated clay particles (Alkaphillic Bacteria and food source)	75			*

labelled sample N. Samples labelled R were produced with a calcium lactate food source at 15 grams per 100m^3 volume and no bacterial spores, while samples labelled BAC consisted of the basic mix, the food source and bacterial spores. These mix designs, shown in Table 1, facilitated the production of three prisms categories. The food source mortar was used for comparison, as the introduction of calcium lactate may affect the performance of the concrete.

Preparation of the clay Liapor (1–4 mm) aggregate samples was carried out by Delft University. This consisted of placing the aggregate in a vacuum, then flooding the aggregate with bacterial spores in a water carrier to impregnate the material with bacterial spores. The healing agent solution contained: calcium lactate (200 g/L), yeast extract (4 g/L) and bacterial spores of the bacillus genus (10^8 spores/L). (Triviloglou et al, 2015)

2.2 Preparation of samples

The prism moulds were filled in two layers and tamped 25 times per layer using a 12 mm × 12 mm square tamping rod in accordance with BS EN 1015-11. To prevent the total fracture of the prism, two steel bars of 1 mm diameter were embedded in the specimen moulds before the mortar was added. The reinforcement bars were fixed 10 mm above the bottom of the mould, with a 20 mm horizontal space between them. Demec gauges as shown in Figure 1 were attached to the sample along the lateral line corresponding to the lower edge of the internal hole running through the sample, and the distance between them was measured using a digital Vernier caliper to determine the crack size at the base of the internal central hole. The crack width on the base was measured directly using Vernier calipers before unloading and after to determine the final size of the crack widths. As can be seen in Figure 1, a central notch was created to ensure the crack occurred at the mid-point.

The reinforced prismatic specimens to be used for the water flow tests were cast with a horizontal hole in the centre of the specimen. This established a conduit from which the water could drain, when determining crack permeability, pre and post healing. The conduit allows water to pass through the full length of the sample and leak from the crack. It was created by casting in a greased smooth bar into the sample, which allowed for easy removal during demoulding.

FIGURE 1. Marked samples prior to crack Induction. Elevation of prism at top.

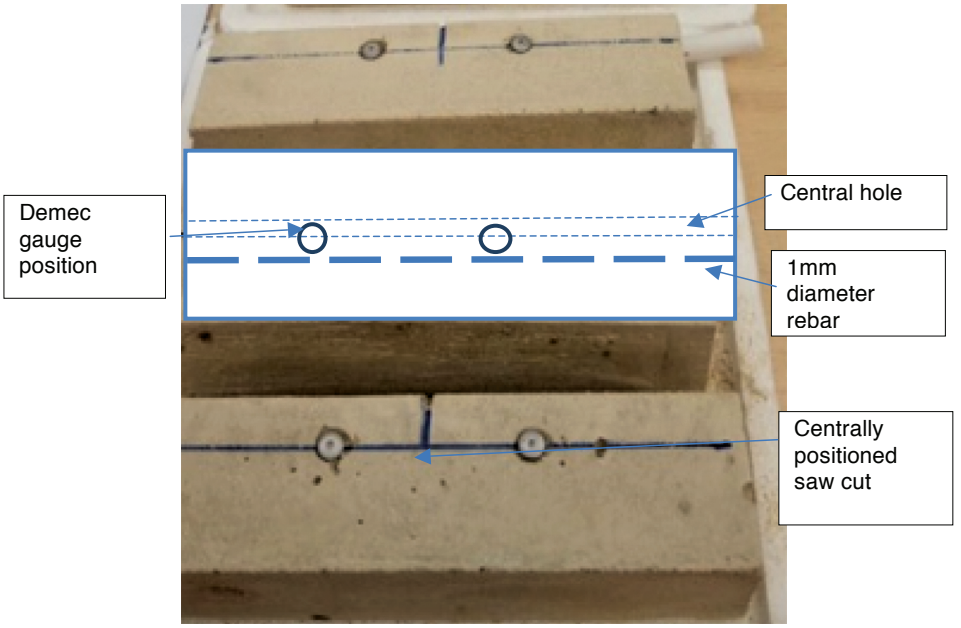

The prism manufacture followed the test standard under development within RILEM TC 235 and detailed by Tzivilogou (2016).

The absorption test samples were cast in the moulds and filled completely with the top surface finished with a steel trowel. Table 2 displays the number of test prisms used within this research; it should be noted that each specimen was used twice. The first time was to determine the water flow, prior to healing, and the second was to determine the degree of sealing/healing due to bacterial action.

2.2.1 Crack creation for the Water Absorption Test and Water Flow Test.

Crack creation to expose the healing agent held within the aggregate was implemented with the use of a 3-point (Lloyds) load/displacement apparatus. The rate of loading used to create the crack was 0.2 mm/min and load was applied until a crack width measuring between 0.2 mm and 0.25 mm was formed. At this point the prism was then unloaded allowing the crack

TABLE 2. Prism production numbers.

Test	BAC	R	N
Absorption	6	6	6
Water flow	8	4	4
Density	3	3	3
Flexural strength			3
Compressive strength			6

to contract. This procedure was repeated on all samples used for the water absorption test and water flow test.

3.0 TEST PROCEDURES

Determination of the capacity for bacteria to heal concrete was assessed using the water test methods, presented in Section 5.1. Section 5.2 present parametric studies in flexural and compressive testing. The surface characteristics of the healed prisms were observed using a 3D Alicona scanner and scanning electron microscopy techniques.

3.1 Water tests

Two water test methods are presented to determine healing capacity. The water flow test examined the post crack permeability of a prism prior to healing and then the healed permeability after 56 days of storage in a water tank. The water absorption test examined the healing capacity in terms of capillary absorption after 56 days of water based storage. Prior to both tests the samples were dried in an environmental chamber.

3.1.1 Water flow test.

The procedure for the water flow test was to set up a water flow static head (500 mm), and place a measuring cylinder under the prism, to collect the residual water flowing through the specimen. The sample was connected to the 5 mm hole running through the sample and one end is sealed using epoxy glue. The test time was 5 minutes from the first drop of water entering the measuring cylinder, shown in Figure 2. The contents of the measuring cylinder were weighed and the result recorded the amount of water that has flowed through the sample in 5 minutes before and after healing. A sealing efficiency calculation was carried out using the change in flow divided by the original flow to express the results as a fraction of a completely sealed crack.

FIGURE. 2 Water Flow during 5 Minute Time Period.

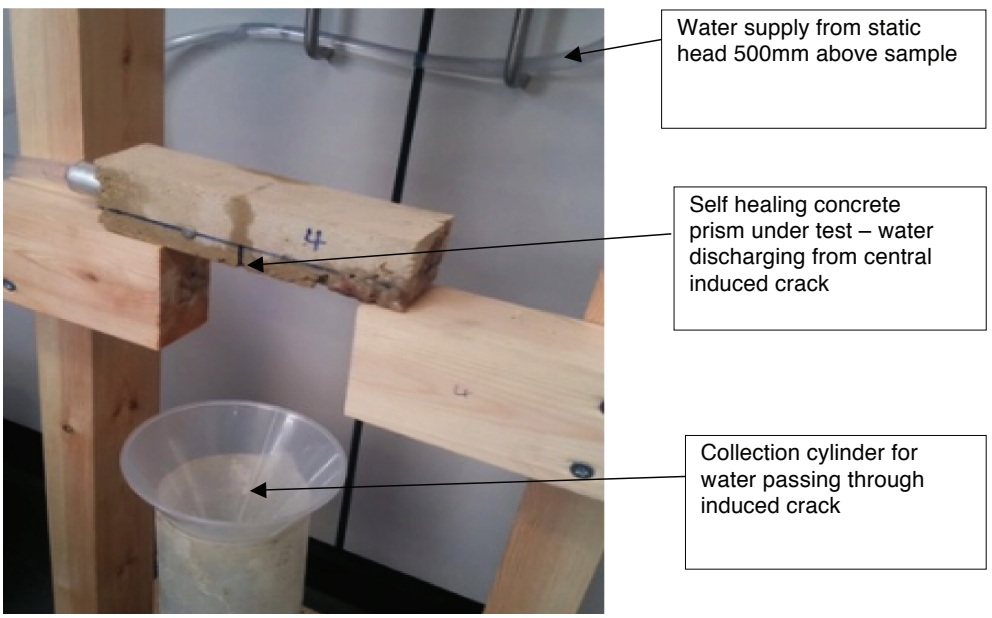

3.1.2 Water absorption test

Figure 3 displays the storage facility of the cracked samples and the test conditions of the dried samples. Testing was carried out after the prisms had been submerged in tanks of water for 56 days. Six samples were tested for each mortar type (N, R, BAC.) All samples were removed from the water 7 days prior to the test being carried out and placed in an environmental chamber. The environmental chamber was set at (40 ± 2)°C with all samples placed in for 7 days to ensure the samples were dry prior to the capillary absorption test. The testing was carried out in an environment with a temperature of 20 ± 1°C.

The water absorption procedure was to fill the test container with 3 mm of water then lay sufficient 3 mm deep spacers into the water to support the samples with the face of the prism in contact with the water. Remove sample from the environmental chamber, weigh the dry weight of each prism and record the data then place the prism into the container on top of the spacer. Weigh the sample frequently in the same order at time periods of: 0.25h, 0.5h, 1h, 2h, 4h, 6h, 8h and record the data, ensuring the water level remains constant.

3.1.3 Post water test prism storage

The water flow samples were subject to an initial timed water flow test and then they were stored for the healing process to occur. The water absorption samples were stored immediately after crack induction. Storage conditions for all prisms used were 20 litre buckets, filled with 5 litres of potable water with three prisms in each covered bucket to prevent evaporation. The prisms were stored for 56 days at 20°C ± 2°C prior to testing.

3.2 Compressive and flexural strength

The flexural strength test was carried out in accordance with BS EN 12390-5:2000, adopting a central point load. Testing to the point of prism breakage under flexure, resulted in the creation of two concrete samples from one prism which were both tested in compression. Compressive strength tests were carried out in accordance with BS EN 12390-3:2009. The area of the half prisms under compression was measured using Vernier callipers, taking the line of best fit across the fracture plane. The half prisms were placed between the platens of an Elle compression testing apparatus, where the load was applied at a rate of 2.4 kN/s until failure. Failure was detected when the load started to drop as the platen moved downwards.

3.3 Alicona and SEM analysis

A 3D optical measurement system (Alicona Infinite Focus G4) was used to examine the surface of the healed crack. The system has a resolution of 40 nm. The measurement system is capable of providing complete 3D information through measurements of X, Y, Z coordinates for millions

FIGURE 3. Section through water tank used for storage and capillary testing.

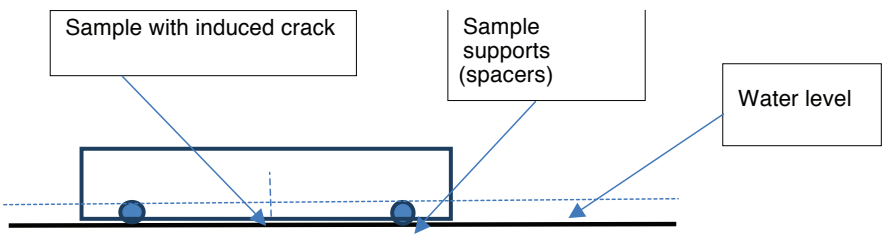

of points on the scanned samples. The data can be presented in either true colour or as a colour graded model.

A scanner was used to visually assess the crack and the degree of healing. The benefit of this system is that it permits large sections of material to be analysed in very fine detail. Scanning electron microscopy complimented by electron dispersive spectrometry was also employed to aid verification of the nature of the precipitate formed from microbial action, as suggested in Section 3.0.

4.0 RESULTS AND DISCUSSION

4.1 Compressive and flexural strength

Results from the compressive and flexural strength tests undertaken on all samples are shown in Table 3. The flexural strength test broke the prism into two parts and each part was tested in compression, therefore sample 1 becomes samples 1.1 and 1.2 following the flexural strength test. The load areas measured prior to calculating the compressive strength are not all equal due to the unpredictable nature of the prism fracture.

There is a link between density and strength as shown in Table 3 and 4. The addition of calcium lactate food source on its own has produced a much denser and stronger concrete than

TABLE 3. Flexural and compressive strength.

Specimen	Strength Test Bacteria Prisms (BAC)	Strength Test R (Food Source) Prisms	Strength Tests Control Prisms (N)
	Flexural Strength (MPa)	Flexural Strength (MPa)	Flexural Strength (MPa)
1	6.3	9.3	5.4
2	6.3	7.3	6.1
3	6.3	9.6	5.4
SD	0.00	1.2	0.4
	Compressive Strength (MPa)	Compressive Strength (MPa)	Compressive Strength (MPa)
1.1	18.1	63.9	26.7
1.2	21.1	73.3	28.9
2.1	15.7	42.3	31.00
2.2	30.8	42.2	29.9
3.1	20.8	54.0	29.2
3.2	27.7	46.9	30.8
Mean	22.4	53.7	29.4
SD	5.8	14.1	1.6

TABLE 4. BAC Bacteria Water Flow Test—physical characteristics.

Bacteria Prism, Water flow test—physical characteristics			
Specimen	Dimensions (H × W × D, mm)	Cross Section Area (mm^2)	Density kg/m^3
1. BAC	41.11 × 39.96 × 160.01	1642.8	1870
2. BAC	41.11 × 39.93 × 161.71	1641.5	1881
3. BAC	40.72 × 39.97 × 160.09	1627.6	1877
1. R	40.80 × 40.04 × 159.54	1633.6	2197
2. R	40.27 × 40.18 × 160.02	1618.1	2116
3. R	39.80 × 40.40 × 160.31	1607.9	2116
1. N	40.31 × 39.92 × 159.88	1609.2	2047
2. N	41.02 × 39.97 × 160.23	1639.6	2085
3. N	40.42 × 40.55 × 160.53	1668.2	2033

plain or bacterial concrete. The impregnation of lightweight bacterial spores into the Liapor aggregate appears to negate the effect of the calcium lactate.

4.2 Water Flow Test

Table 4 displays the physical characteristics of the prisms under test. There is a noticeable difference between the BAC prism density and the N control sample density. This is due to the lightweight Liapor clay aggregate.

Results from the water flow tests undertaken on all sample types are shown in Tables 5, 6, and 7. Sealing efficiency was calculated by subtracting the final flow from the initial and dividing by the initial flow.

It should be noted that while some aggregates will rupture, on crack propagation, others will remain intact as the crack propagates around the capsule. Where fewer aggregates rupture, less bacteria is available to react with the catalyst to create calcium carbonate. However, Table 7, illustrates a significant healing efficiency of 85% when compared to the control sample: significance was determined using a paired comparison "T" test and the results were interrogated using a paired t-Test. For all of the results produced the confidence intervals have been set at 95%. The results comparing the control sample with the healed sample presented the following: P Value, 0.000799 this is <0.05 therefore, reject the null Hypothesis and accept the alternative hypothesis.

Table 6 illustrates the results from the water flow test that were carried out on the R (Food Source) prisms before and after the healing process had taken place. A small amount of autogenous healing appears to have taken place in samples 1 and 3, however, the negative value marked with an asterisk has been removed from the average and standard deviation values.

Table 7 shows the results from the water flow test carried out on the control prism samples. The results from the water flow testing of samples 2 and 4 did suggest that these samples had

TABLE 5. BAC Bacteria Prism Water Flow Test.

Specimen BAC	Peak load (kN)	Crack Width At The Side	Crack width at the bottom	Initial water flow (g)	Final water flow (g)	Sealing efficiency (%)
1.	2.71	0.35 mm	0.75 mm	322.5	90.3	72.0
2.	2.34	0.25 mm	0.40 mm	289.2	86.1	70.3
3.	2.25	0.26 mm	0.40 mm	1012.5	74.2	92.7
4.	2.12	0.19 mm	0.55 mm	235.6	43.9	81.4
5.	2.42	0.22 mm	0.33 mm	822.1	82.0	90.0
6.	2.36	0.18 mm	0.30 mm	1560.4	185.0	88.2
7.	2.15	0.40 mm	0.50 mm	2240.2	83.2	96.3
8.	2.15	0.19 mm	0.30 mm	795.4	52.2	93.4
					Average healing %	85.5
					Standard Deviation	9.3

sealed under a process of autogenous healing, since no bacteria was present in these batches. Sample 1 shows no significant change, while sample 3 produced a much greater final flow volume as marked with an asterisk, this has been removed from the result analysis. This could be due to man-handling of the specimens and dislodging small fragments of broken material at the rupture plane.

TABLE 6. R Food Source Prism Water Flow Test Results.

R Food Source Prism Water flow test					
Specimen R	Peak Load (kN)	Crack width at the side surface	Initial Water Flow (g)	Final water flow (g)	Sealing Efficiency (%)
1.	3.13	0.22 mm	201.8	53.3	73.2
2.	3.34	0.19 mm	50.4	38.0	22.4
3.	4.432	0.3 mm	205.1	73.1	64.4
4.	1.81	0.22 mm	33.1	57.1	–57.1*
				Average healing %	53.3
				Standard Deviation	27.15

TABLE 7. N Control Prism Water Flow Test Result.

Control Prism Water flow test					
Specimen N	Peak load (kN)	Crack width at the side surface	Initial water flow (g)	Final water flow (g)	Sealing Efficiency (%)
1	2.23	0.22 mm	248.87	271.26	–9.02
2	1.65	0.20 mm	132.05	46.34	64.91
3	2.26	0.19 mm	78.36	173.9	–121.92*
4	2.02	0.26 mm	1073.4	652.84	39.18
				Average Sealing %	47.5
				Standard Deviation	34.50

Figure 4 illustrates the self-healing efficiency of the three prism types and the self healing ability of the prisms with a bacteria inclusion is self evident.

4.3 Water Absorption Test

Results from the water absorption tests undertaken on all samples are shown in Tables 10, 11, and 12. Figure 5 shows a comparison of the mean water absorption over an 8-hour period of each sample batch.

FIGURE 4. healing efficiency of prisms.

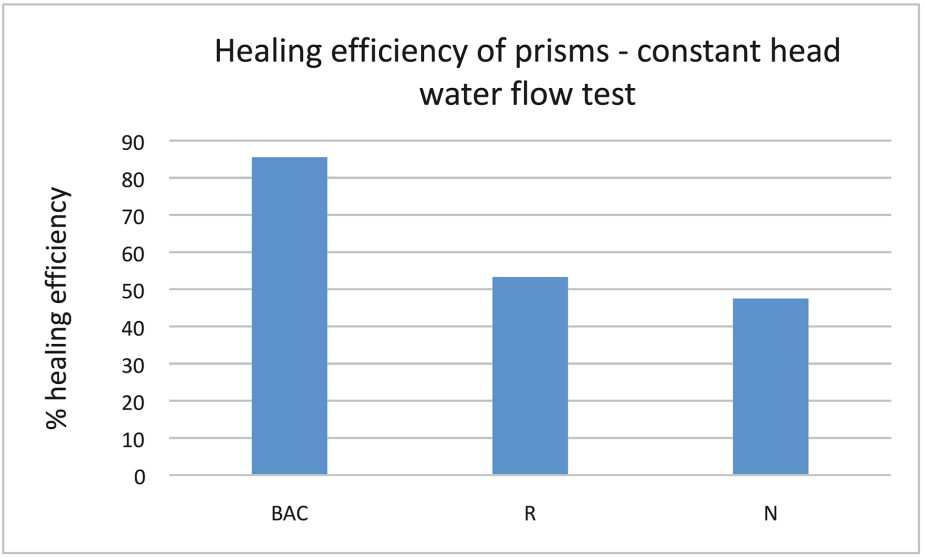

TABLE 10. BAC Bacteria and Food Source Prism Water Absorption Results.

BAC Bacteria and Food Source Prism Water Absorption Without Bottom Sealed								
Ref BAC	Initial dry weight (g)	after 0.25h	after 0.5h	after 1h	after 2h	after 4h	after 6h	after 8h
1.	482.09	486.37	485.58	486.74	487.58	488.59	489.68	489.96
2.	483.89	487.72	486.56	487.96	488.78	489.64	490.31	490.99
3.	489.9	491.45	490.95	491.88	492.84	493.54	494.31	495.075
4.	483.22	485.51	484.9	485.98	486.8	487.43	488.1	488.76
5.	485.98	488.79	488.2	489.21	490.56	491.16	491.75	492.63
6.	489.95	492.35	492.18	492.84	493.91	494.47	494.93	493.78
Average	485.38	488.70	488.06	489.10	490.08	490.81	491.51	491.86
S D	3.41	2.74	2.96	2.77	2.87	2.78	2.68	2.39

Table 10 shows the results from the water absorption test carried out on bacteria & food prisms at various time intervals.

Table 12 presents the results of the water absorption test carried out on the N prisms.

Table 12 shows the results of the water absorption test carried out on the control prisms.

TABLE 11. R Food Source Prism Water Absorption Results.

R (Food Source) Prism Water Absorption Without Bottom Sealed								
Specimen R	Initial dry weight (g)	after 0.25h	after 0.5h	after 1h	after 2h	after 4h	after 6h	after 8h
1.	523.18	525.51	525.96	526.03	526.98	527.85	528.98	530.15
2.	514.84	516.75	517.15	518.2	519.15	520.14	521.35	522.86
3.	521.36	523.31	523.18	523.74	524.12	525.16	525.89	527.65
4.	513.74	516.49	517.64	518.61	520.7	522.56	524.02	524.86
5.	520.05	523.5	525.49	527.07	529.14	531.41	532.11	533.62
6.	517.17	521.11	521.86	524.68	527.35	530.39	531.85	531.82
Average	518.39	521.11	521.88	523.06	524.57	526.25	527.37	528.49
Standard Dev	3.75	3.75	3.79	3.78	3.97	4.44	4.35	4.14
Weight Increase	0	2.49	2.72	3.67	6.18	7.86	8.98	10.1

TABLE 12. N Control Prism Water Absorption Test Results.

N Control Prism Water Absorption Without Bottom Sealed								
Specimen N	initial dry weight (g)	after 0.25h	after 0.5h	after 1h	after 2h	after 4h	after 6h	after 8h
1.	554.86	559.21	559.65	561.05	562.45	564.15	565.46	566.03
2.	547.69	552.29	552.7	553.93	555.12	557.05	558	559.21
3.	545.05	550.02	550.23	551.24	552.96	553.95	555.15	556.61
4.	554.09	558.18	558.63	559.76	561.11	562.92	564.5	566.7
5.	558.1	561.87	562.61	562.95	564.36	565.59	566.89	568.01
6.	551.12	554.61	555.89	556.47	557.8	558.77	560.02	561.27
Average	551.81	556.03	556.61	557.56	558.96	560.40	561.67	562.97
Standard Dev	4.84	4.49	4.60	4.48	4.43	4.53	4.65	4.61
Weight Increase	0	4.22	4.80	5.75	7.15	8.59	9.86	11.16

The logarithmic comparison between the average amounts of water absorbed over an 8 hour period by each prism type is displayed in Figure 5. The absorption process was a combination of capillary action in the induced crack and pore structure within the cementitous materials. The BAC prism absorbed the least amount of water. All samples show a reduction in the rate of water absorption over time, in line with the logarithmic progression.

FIGURE 5. Logarithmic Water Absorption Comparison Graph.

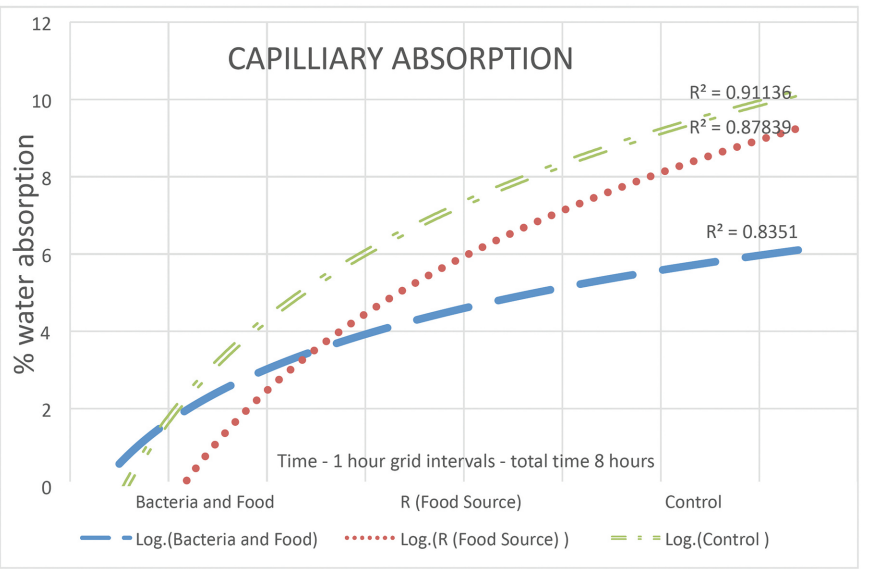

The control sample, which produced the largest volume of water flow also performed the least well in the water absorption test. The Control Prism absorbed 43% more water over the eight-hour period in comparison with the bacteria and food prism.

This suggests that water ingression on concrete structures would be reduced by using bacterial concrete. In turn, this would reduce the maintenance required on the building. However further testing needs to be conducted in, areas where all of the micro-capsules have been ruptured which will develop the theory presented by Trask, (2007).

4.4 Alicona scan of healed crack

Using the Alicona software, Figure 6 presents an image of a healed fracture for a bacterial prism. The white material as shown is the calcium carbonate within the induced crack. The dark edge is the original mortar. Using the Alicona software a 3D scan of the same fracture is shown in Figure 7. The 3D image/scan shows the different levels of material bridging indicating material healing about the fracture plane. The sample has been healed due to the bacteria producing calcium carbonate sealing the crack. This in turn has resulted in a reduced water flow.

Figure 8 shows the depth of the partly healed fracture in graph form, which is displayed in Figure 7 as the central colour coded crack. Using the scale of colour contours it was observed that the crack was sealed to within 0.8 mm of the surface of the prism. This shows healing to near the full crack depth of the original 20 mm fracture depth. The effect of the healing agent can be clearly observed running vertically in the centre section of the Alicona scan in both Figures 7 and 8.

4.5 Electron Dispersive Spectroscopy (EDS) Composition Results

The formation of the precipitate in the fracture zone was analysed using the EDS part of the SEM as displayed in Figure 8. This produces a breakdown of the elements within the precipitate

FIGURE 6. Alicona Scan of Bacteria sealed fracture section.

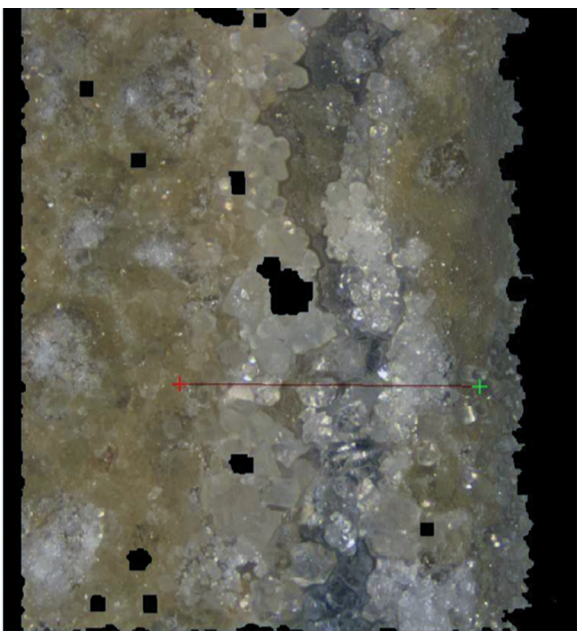

FIGURE 7. Alicona scan of Bacteria 3D Fracture Model.

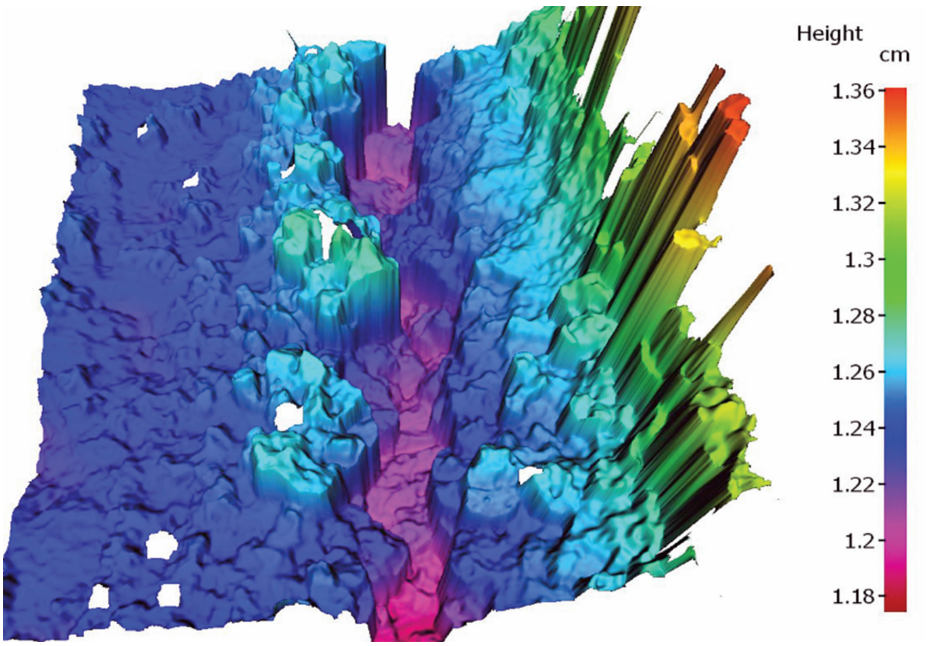

FIGURE 8. Alicona—Bacteria Prism 2D Fracture Depth Graph.

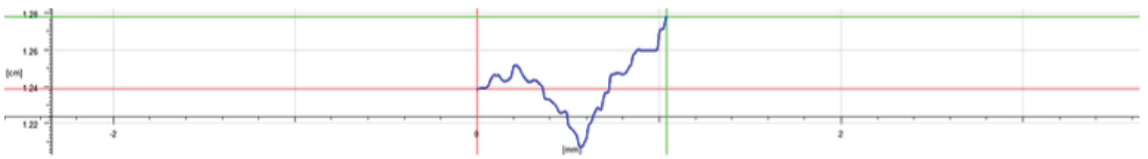

ReferencePosition	l: 1.0412mm	z: 1.2785cm
MeasurePosition	l: 0.0000nm	z: 1.2386cm
RelativeMeasurement	Δl: -1.0412mm	Δz: -399.2775µm
	Angle: 200.9813°	Distance: 1.1151mm
Filter:	No Filter - Primary profile	

and their relative percentages present. The EDS composition results facilitates precipitate categorisation relative to the design mix adopted.

Figure 7 suggests the presence of high levels of carbon and oxygen with lower levels of calcium, indicating the formation of calcium carbonate in the rupture plane of the healed material.

5.0 CONCLUSION

When comparing the water flow test and the capilliary absorption test procedures, both procedures provided complimentary results, as can be seen by comparing Figures 3 and 4. The formation of the cracks, induced for healing can only be observed at the external face and it cannot be known whether or not the crack divides once or more internally. The water flow test

FIGURE 9. Bacteria & Food Prism Atomic Composition.

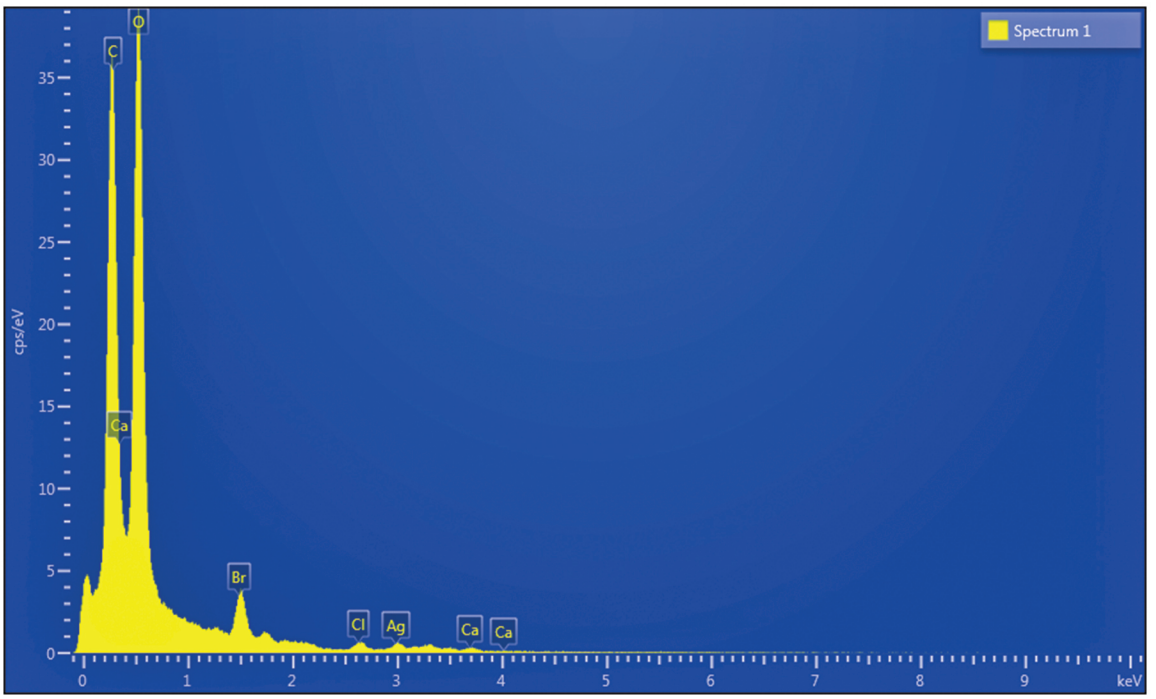

is not as sensitive to this phenomenon; as a force of water is applied at a constant head and accurate sealing efficiency can be measured, following the initial flow test to provide a benchmark against a perfectly sealed specimen. However, the test relying upon capillary absorption may be greatly affected by the initial crack sub dividing into two or more internal fractures. This will dramatically increase the tendency for capillary suction to occur and may skew the results. In addition the induced crack provided for capillary absorption does not have a value to compare the percentage healing against The water flow test has provided the safest and most practical test that could be commercially adopted due to its ease of operation, lack of variables that may skew the final results. We would recommend this be an adopted test for self healing materials.

It can be concluded that the addition of bacterial aggregates to concrete prisms does allow self-healing to occur, after fracture which corroborates work carried out by Tziviloglou et al, (2016a). The creation of calcium carbonate through precipitation seals the fracture, reducing the water flow and water absorption, thus improving durability. The fracture zones may not be fully filled with calcium carbonate but a large degree of self healing has taken place. A surface treatment to seal the residual cracks may be an additional environmentally friendly treatment that can be used to completely seal the fracture (Richardson et al 2014 and 2016). A key advantage of this method of crack healing in concrete, is the use of an environmentally friendly bacteria with no side effects or that is capable of any environmental damage. It is a very clean process without high manufacturing costs and no environmentally unfriendly chemicals have been used in the production of the materials required for this repair system.

5.1 Further Work

The crack healing capability of concrete is required at the surface. The cost of creating self healing material is higher than plain concrete. It is therefore recommended that a full size trial

be undertaken using self healing pre-cast concrete panels at the thickness of the required cover, to act as a permanent formwork and external self healing protection to the structure. This would permit a full strength concrete to be used where it is needed within the structural section and obliviate the need for self healing materials to be placed at the centre of the structural element, thus maximising the cost benefit ratio.

Work by Grumbein et al (2016) has shown that with the use of bio films, the surface of the concrete or cementitous mortar can be made to be hydrophobic. This is an area for further research to create a complimentary strategy for self healing concrete material.

Acknowledgements

Ghent University for providing ready-made prism samples for absorption tests. Delft University for providing the prepared Liapor aggregate and general thanks to all of the members of RILEM TC 253-MCI.

6.0 REFERENCES

Barbero-Barrera, M. del M, Maldonado-Ramos, L., Van Balen, K., García-Santos, A., and Javier Neila-Gonzáleza, F. (2013). Lime Render Layers: An Overview of Their Properties, *Journal of Cultural Heritage*, 15, pp. 326–330.

Brown A.J. (1886). The chemical action of pure cultivations of bacterium aceti. Journal Chem Soc, Vol 49, pp. 432–439.

BS EN 1015-11:1999. *Methods of test for mortar for masonry*, London: British Standards Institute.

BS EN 12390-2:2009. *Testing hardened concrete. Making and curing specimens for strength tests*, London: British Standards Institute.

BS EN 12390-3:2009. *Testing hardened concrete. Compressive strength of test specimens*, London: British Standards Institute.

BS EN 1992-3:2006. Euro code 2, *Design of concrete*, London: British Standards Institute.

Farrell, P., Sheratt, F., and Richardson, A. (2016). *Writing Built Environment Dissertations and Projects: Practical Guidance and Examples*, Wiley Blackwell, UK

Gollapudi, U.K., Knutson, C.L., Bang, S.S., and Islam, M.R. (1995). A new method for controlling leaching through permeable channels, *Chemosphere*, 30(4), pp. 695–705.

Grumbein, S., Minev, D., Tallawi, M., Boettcher, K., Prade, F., Pfeiffer, F., Grosse, C.U., and Lieleg. O. (2016), Hydrophobic Properties of Biofilm-Enriched Hybrid Mortar, *Advanced Materials*, Vol 28, pp. 8138–8143.

Jonkers, H.M., Thijssen, A., Muyzer, G., Corpuroglu, O., and Schlagen, E. (2010). Application of bacteria as self healing agent for the development of self healing concrete, *Ecological Engineering*, Vol 36, pp. 230–235.

Matsuoka, M., Tsuchida, T., Matsushita, K., Adachi, O., and Yoshinaga, F. (1996). A synthetic medium for bacterial cellulose production by Acetobacter xylinumsubsp.sucrofermentans, *Bioscience, Biotechnology, and Biochemistry*, 60(4), pp. 575–579. doi: 10.1271/bbb.60.575.

Pacheco-Torgal, F., and Labrincha, J.A. (2013). Biotech cementitious materials: Some aspects of an innovative approach for concrete with enhanced durability, *Construction and Building Materials*, 40, pp. 1136–1141. doi: 10.1016/j.conbuildmat.2012.09.080.

Richardson, A., Coventry, K., and Pasley, J. (2016). Micro-induced calcite precipitation—crack sealing application, The 9th International Concrete Conference, Environment, Efficiency and Economic Challenges for Concrete, Dundee University, UK, July 4–6, pp. 30–36.

Richardson, A.E., Coventry, K.A., Forster, A., and Jamison, C. (2014). Surface consolidation of natural stone materials using microbial induced calcite precipitation, *Structural Survey*, Vol. 32, Iss: 3, pp. 265–278.

Schramm, D., Shamp, A., and Zumbach, D. (2004). *A report on Concrete Sealants With Emphasis on Their Radon Blocking Capabilities and Their Green Values*. Available at: http://www.stolaf.edu/people/jackson/08-124/gbreport/ConcreteSeal_J04.pdf (Accessed: 1 November 2016).

Trask, R.S., Williams, H.R., and Bond, I.P. (2007). Self-healing polymer composites: Mimicking nature to enhance performance, journal. doi: 10.1088/1748-3182/2/1/p01.

Tzivilogou, E., Wicktor, V., Jonkers, H.M., and Schlangen, E. (2015). Development of bio-based self healing concrete to increase durability of structures, eighth International Conference on Construction in the 21st century (CITC-V111), Changing the field: Recent developments for future Engineering and construction, May 27–30, Thessalonica, Greece.

Tziviloglou, E., Wiktor, V., Wang, J., Paine, K., Alazhari, M., Richardson, A., Gueguen, M., De Belie, N., Schlangen, E., and Jonkers, H. (2016a). "Evaluation of experimental methodology to assess the sealing efficiency of bacteria based self healing mortar: Round robin test." Delft, Netherlands.

Wiktor, V., and Jonkers, H.M. (2011). Quantification of crack-healing in novel bacteria-based self-healing concrete, *Cement and Concrete Composites*, 33(7), pp. 763–770. doi: 10.1016/j.cemconcomp.2011.03.012.

Wu, M., Johannesson, B., and Geiker, M. (2012). A review: Self-healing in cementitious materials and engineered cementitious composite as a self-healing material, *Construction and Building Materials*, 28(1), pp. 571–583. doi: 10.1016/j.conbuildmat.2011.08.086.